Two-section branch-line hybrid couplers based broadband transmit/receive switch

Ashraf Abuelhaija[1], Gameel Saleh[2]
[1]Department of Electrical Engineering, Applied Science Private University, Amman, Jordan
[2]Department of Biomedical Engineering, College of Engineering, Imam Abdulrahman Bin Faisal University, Dammam, Saudi Arabia

Article Info

Article history:

Received Jun 1, 2022
Revised Sep 7, 2022
Accepted Oct 1, 2022

Keywords:

Harmonic frequency
Hybrid coupler
Insertion loss
Magnetic resonance imaging
Transmit/receive switch

ABSTRACT

This article introduces a broadband microstripline-based transmit/receive switch for 7-Tesla magnetic resonance imaging. The designed switch aims to handle a signal of multiple frequencies to/from a multi-tuned radio-frequency coil that resonates at frequencies corresponding to the speed of precession of a wide range of atomic X-nuclei, at the same time and without tuning. These include 1H, 23Na, 13C, 31P, 19F, and 7Li used in magnetic resonance spectroscopy as a measure to the existence of many diseases. The fundamental and third harmonic center frequencies of the switch are adjusted to resonate at two broadbands covering a wide range of atomic X-nuclei. Two section branch-line hybrid couplers with phase inverters are designed to build the broadband switch. The designed switch used the minimum trace widths of transmission lines that reveal a compact size without increasing the heat and then the loss beyond specific values. The couplers and the switch S-parameters exhibited good return loss (<-10 dB), high isolation (<-40 dB), less insertion loss (<1 dB) and two clear wide bands covering many atomic X-nuclei used in diagnosis, at the same time and without the need for any tuning circuit during operation.

Corresponding Author:

Ashraf Abuelhaija
Department of Electrical Engineering, Applied Science Private University
Amman, Jordan
Email: a_abualhijaa@asu.edu.jo

1. INTRODUCTION

Transmit/receive (T/R) switches in magnetic resonance imaging (MRI) are essential elements when T/R radio frequency (RF) coils are used. They are located between the RF amplifier and the RF coils. The long cables between the power amplifier and the coil as well as the T/R switches add loss to the RF transmitting chain of magnetic for MRI scanner, and thus effect on the power delivered to the transmit coil and increase the noises. The cable loss is reduced by designing power amplifiers of nonmagnetic components near to the magnet bore [1]. Another approach is to design T/R switches that satisfy low insertion loss, high isolation, and good return loss. For single resonant frequency coils, such as 1H protons RF coils, the same single resonance signal must be handled by the switch to the RF coil during transmit and from the coil to the receiver during receive. Similarly, dual and multi resonance T/R RF coils need dual and multi tuned T/R switches, respectively.

Magnetic resonance imaging and spectroscopy (MRI/MRS) can provide images with anatomical and metabolic information of the human [2]–[5]. Several studies have shown that non-proton (X-) nuclear imaging can provide valuable information from tissues [6], [7]. For example, 23Na imaging can examine multiple sclerosis and tumors [8], [9]. 31P imaging has been used for assessing healthy human brain, examine breast cancer and providing complementary information on the biology of prostate cancer [10]–[12]. In this context, several dual-nuclear RF coils have been developed for ultra-high field MRI. In [13], multi-channel 1H/31P RF coil for 7T MRI has been presented. The coil has been designed using a four-channel dipole array for 1H imaging and a four-channel loop array for 31P imaging. In [14], a 1H/23Na RF coil has been presented. This coil is designed using monopole , for 1H imaging, crossing the center of the loop coil, which is used for 23Na imaging.

In the literature, various types of switches have been designed. PIN diodes-based T/R switches are introduced to satisfy high reliability, power handling, linearity [15]–[18]. The switching time from transmit to receive was revealed within 0.4 μs and from receive to transmit reached within 2 μs [16]. Transistors-based T/R switches are introduced in [19], [20]. The enhanced mode eGaN FETs in [16] showed an advantage over PIN diodes in B0 and B1 homogeneity and the amount of biased power to work, but it revealed less image SNR. Micro electromechanical system (MEMS) based switches [21], [22] were designed and compared to topologies based on PIN diodes and they showed higher isolation, and lower DC switching voltage. These switches have not been broadly used in MRI applications.

A novel microstripline (MSL) based T/R switches, for 1H protons 7-Tesla MRI, have been designed and introduced in [23]. In that work, we introduced two switches of unsymmetrical and symmetrical hybrid couplers topologies and compared their results with a third commercial coupler switch from the market. The measurements showed that the MSL-based switches are better in terms of heat dissipation, handling higher power, and have less insertion loss. We introduced new MSL-based T/R switches with different topologies and realistic trace widths to handle the RF pulses to/from 1H RF coils working at 298 MHz, the operating frequency at 7-Tesla MRI [24]. The introduced switch achieves a compact design with minimum dimensions and without increasing the temperature 20 degree Celsius beyond the ambient temperature. Dual tuned MSL-based T/R switches have also been introduced to work properly with dual resonance RF coils to interrogate different X-nuclei [25]. Our proposed and introduced microstripline-based switches can handle the RF pulses, with very low insertion loss, as well as good return loss and isolation, to/from single and dual tuned RF coils.

In this article, a new broadband MSL-based T/R switch is designed to handle RF pulses of multiple resonances to/from multi-tuned RF coils, at the same time and without tuning. These resonances are falling within two broadbands where the speed of various X-nuclei (such as 1H, 23Na, 13C, 31P, 7Li, 19F) exist. The targeted atomic X-nuclei are used in magnetic resonance spectroscopy (MRS) as a measure to the existence of many diseases. The objective of this work is to achieve this broadband design, reduce the insertion loss, minimize the size while keeping the realistic design constraints of trace widths and its allowable maximum acceptable temperature.

2. METHODS AND MATERIALS

The two-section branch-line broadband hybrid coupler has been originally presented in [26]. It consists of three vertical transmission lines (a,c,a) and four horizontal transmission lines (b,b,b,b) as shown in Figure 1. An inverter (180° phase shifter) has been inserted at the middle vertical transmission line to enhance the bandwidth. The length for all the transmission lines is the same and equal to quarter wavelength.

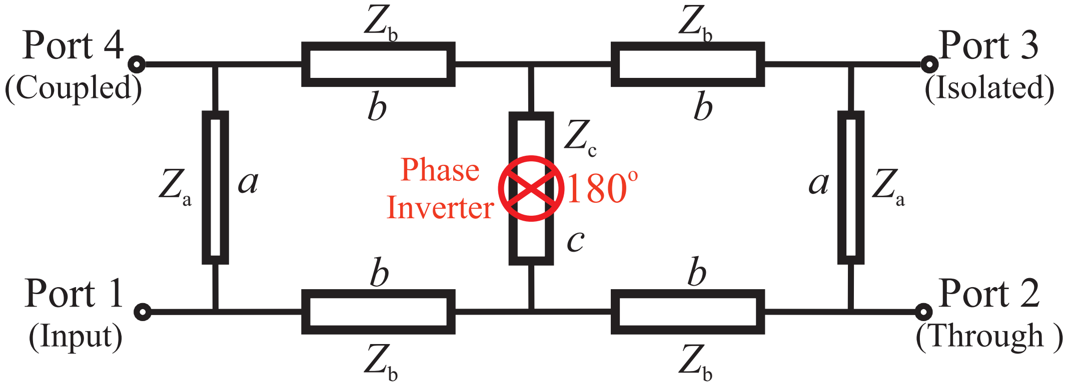

Figure 1. Schematic diagram of the two-section branch-line hybrid coupler

The scattering matrix of this hybrid coupler has been derived in [27], and can be presented as (1):

$$\begin{pmatrix} S11 & S12 & S13 & S14 \\ S21 & S22 & S23 & S24 \\ S31 & S32 & S33 & S34 \\ S41 & S42 & S43 & S44 \end{pmatrix} = \begin{pmatrix} 0 & -\sqrt{(\frac{k}{k+1})} & 0 & -j\sqrt{(\frac{1}{k+1})} \\ -\sqrt{(\frac{k}{k+1})} & 0 & -j\sqrt{(\frac{1}{k+1})} & 0 \\ 0 & -j\sqrt{(\frac{1}{k+1})} & 0 & -\sqrt{(\frac{k}{k+1})} \\ -j\sqrt{(\frac{1}{k+1})} & 0 & -\sqrt{(\frac{k}{k+1})} & 0 \end{pmatrix} \tag{1}$$

where "k" is the ratio of the signal power at the through port to the signal power at the coupled port, and can be expressed as (2):

$$k = \left|\frac{S21}{S41}\right|^2 = \frac{Z_o^2 Z_c^2}{Z_b^2} \tag{2}$$

where Z_c and Z_b are the characteristic impedances for transmission lines "c" and "b", respectively. To calculate these impedances together with the characteristic impedances for the transmission line "a" (Z_a), we can use (3) and (4):

$$Z_a = (\sqrt{k} + \sqrt{k+1})Z_o \tag{3}$$

$$Z_c = \frac{\sqrt{k}Z_b^2}{Z_o} \tag{4}$$

In order to obtain the quadrature hybrid coupler with -3 dB output ports, the ratio "k" should be equal to 1. In this case, the input RF signal is inserted into port 1. Port 2 (through) and port 4 (coupled) are the -3 dB quadrature outputs. Port 3 is the isolated port. Now, if we assume Z_b=Z_o, then Z_c will be equal to Z_o from (4), and Z_a will be equal to 2.414 Z_o from (3). This hybrid coupler has been designed on Rogers substrate RO 4,725 with relative permittivity 2 55 and thickness of 1.542 mm using ADS software, as shown in Figure 2. The dimensions of the final design are 400×180 mm.

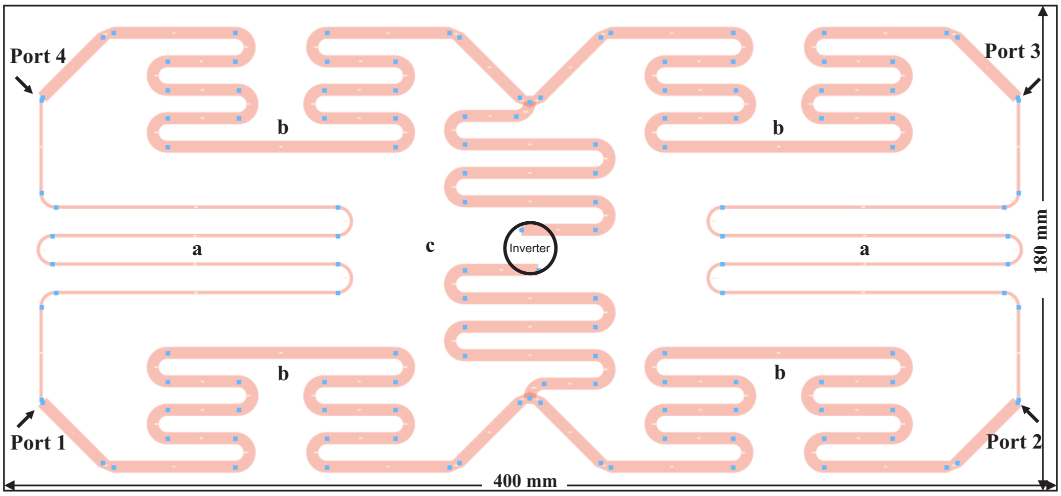

Figure 2. Layout of the two-section branch-line hybrid coupler

In order to build-up the broadband T/R switch using the two-section branch-line hybrid couplers, the connections shown in Figure 3 have been applied. If we imagine a virtual line between the two couplers acting as a mirror, then the two hybrid couplers are connected to each other at two ports: the through ports and the coupled ports. At transmit, the two PIN diodes which are connected at through and coupled ports of the first coupler (left), are forward biased. In this case, all the input signals will be delivered to the RF coil at port 2. At receiving, both PIN diodes are reverse biased and the detected RF signal from the RF coil at port 2 will be delivered to port 4.

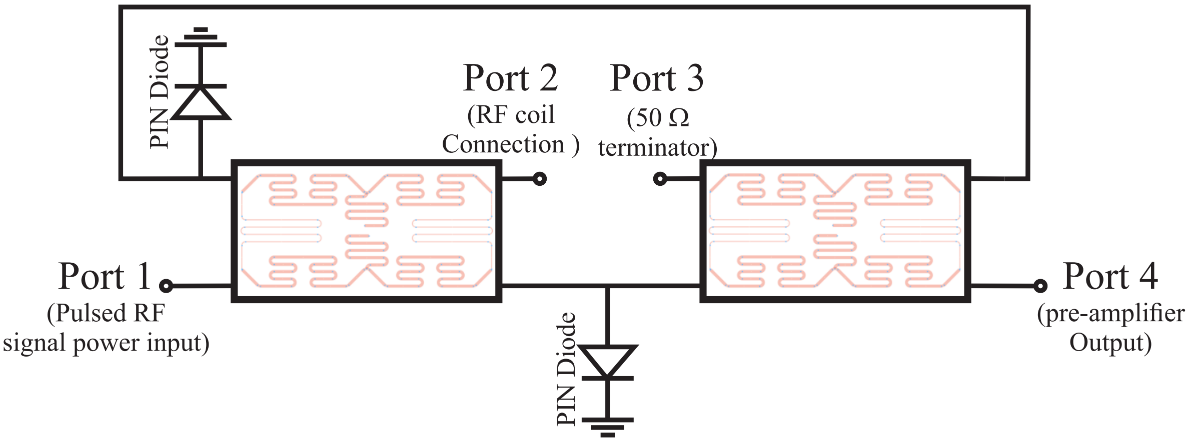

Figure 3. Two-section branch-line hybrid couplers based broadband T/R switch

Two short coaxial cables are used to operate as inverters at the middle transmission line of each coupler. A 180° phase shift can be achieved using coaxial cable once the straight connection is replaced by a crossover connection as shown in Figure 4. The first coaxial cable is inserted between ports 9 and 10 whereas the second coaxial cable is inserted between ports 11 and 12.

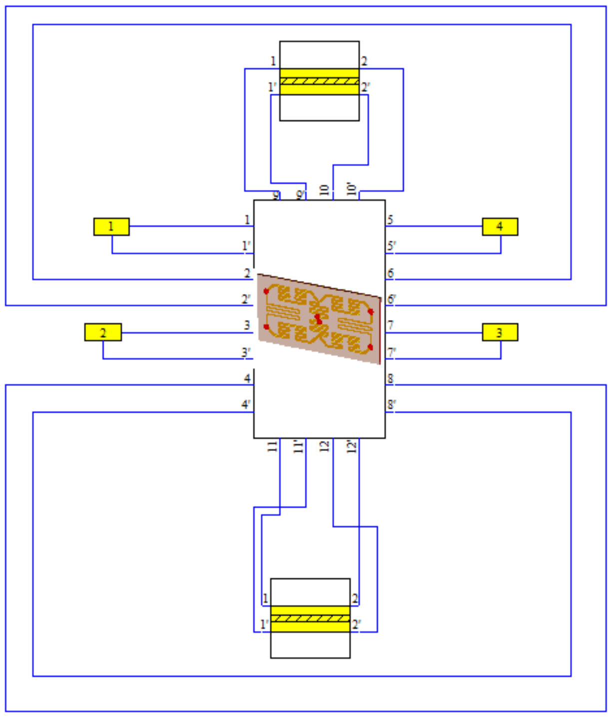

Figure 4. The broadband T/R switch in CST showing the connections of ports and the two inverters (cross connected coaxial cables)

3. RESULTS AND DISCUSSION

The designed two-section branch-line hybrid couplers as shown in Figure 2 characterized by two broadbands appear at the fundamental frequency and the third odd harmonics, as shown in Figure 5. This Figure demonstrates good return loss and isolation. The bandwidths of the first and second broadband were falling in the ranges 75-135 MHz and 293-334 MHz. These broad bandwidths have been specified based on the definition of the coupling imbalance between the two output ports (through and coupled) that must be better than 0.86 dB (3.0 ± 0.43 dB) [28].

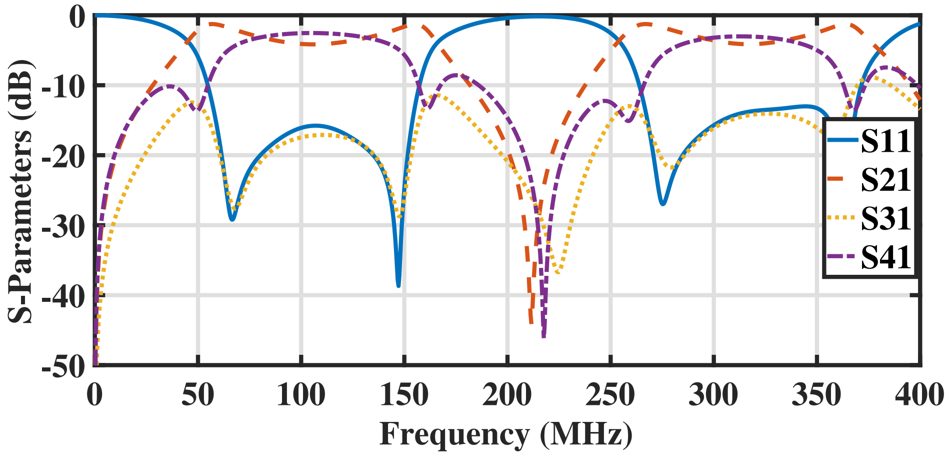

Figure 5. S-parameters for the two-section branch-line hybrid couplers

To evaluate the performance of the proposed two-section branch-line hybrid couplers based broadband T/R switch, S-parameters have been obtained from CST. At transmit, good matching (S11< -10 dB) and low insertion loss (S21< -1dB) have been obtained at all atomic nuclei resonance frequencies, as shown in Figure 6 and Table 1. In addition, high isolation (S41< -40 dB) between transmitter and receiver can be obtained.

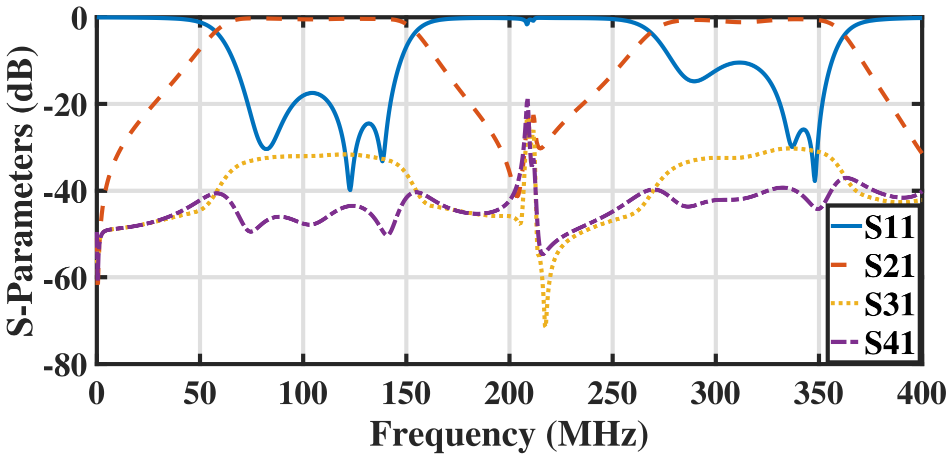

Figure 6. S-parameters at transmit phase for two-section branch-line hybrid couplers based broadband T/R switch

Table 1. S-parameters for two-section branch-line hybrid couplers based broadband T/R switch at transmit phase

Atomic Nuclei	Frequency (MHz)	S11 (dB)	S21 (dB)	S41(dB)
13C	75.0	-23.2	-0.25	-50
23Na	78.8	-28.7	-0.26	-48
7Li	115.8	-22.6	-0.38	-45
31P	120.6	-32.1	-0.35	-44
19F	280.4	-11.2	-0.92	-42
1H	298.0	-13.0	-0.74	-42

At receiving, good matching (S22< -13 dB) and low insertion loss (S21< -0.9 dB) have been obtained at all atomic nuclei resonance frequencies, as shown in Figure 7 and Table 2. It is worth to mentioning that the first operating band of the T/R switch is extended from 66.2-147.3 MHz. Whereas the second operating band is extended from 279.6-352.2 MHz. Within these two bands, an insertion loss is lower than 1 dB and the return loss is at least 10 dB can be obtained at both transmit and receive modes.

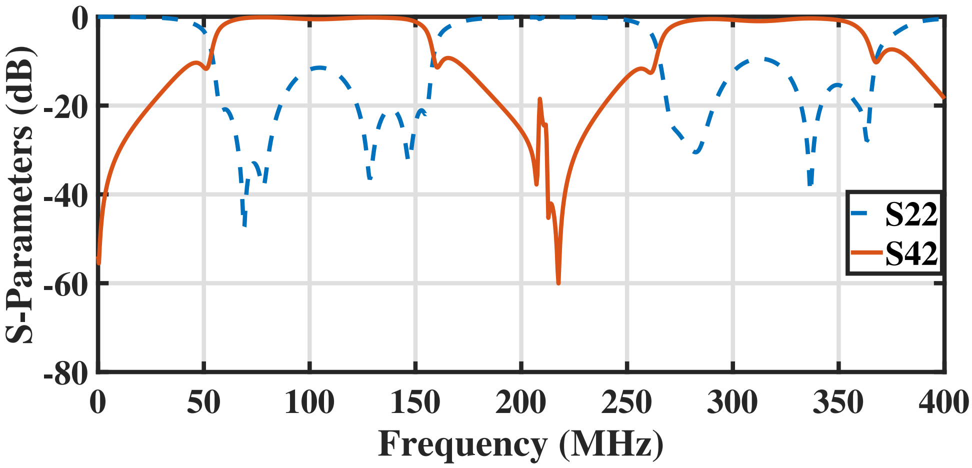

Figure 7. S-parameters at receive for two-section branch-line hybrid couplers based broadband T/R switch

Table 2. S-parameters for two-section branch-line hybrid couplers based broadband T/R switch at receive phase

Atomic Nuclei	Frequency (MHz)	S22 (dB)	S24 (dB)
13C	75.0	-33.6	-0.15
23Na	78.8	-37.1	-0.12
7Li	115.8	-14.1	-0.37
31P	120.6	-17.8	-0.26
19F	280.4	-30.0	-0.83
1H	298.0	-13.6	-0.61

4. CONCLUSION

In this work, a transmit/receive switch is designed to handle a broadband signal of operating frequencies to/from multi-tuned radio-frequency coil working at 7-Tesla MRI. The two-section branch-line method is used from transmission line theory to design two stacked microstripline-based hybrid couplers of two broadband signals covering many atomic X-nuclei. The couplers and then the switch have been designed using ADS and MW-CST. The broadband couplers have been designed with an excellent coupling imbalance between the two output ports, (3.0 $\pm$ 0.43 dB), that satisfies bandwidth of 75–135 MHz and 293-334 MHz. The proposed broadband T/R switch achieved good matching (S11< -10 dB) and low insertion loss (S21<-1 dB) at transmit, and high isolation (S41<-40 dB) between transmitter and receiver. At receiving, the switch revealed good matching (S22< -13 dB) and low insertion loss (S21< -0.9 dB). These values have achieved at two wide broadbands of operating frequencies (from 66.2 to 147.3 MHz and from 279.6 to 352.2 MHz.) covering many atomic X-nuclei including the 32Na, 31P, 13C, 19F, 7Li and others as well as the 1H. These bandwidths have been calculated based on achieving an insertion loss less than 1 dB and a return loss better than 10 dB. Our broadband switch can work with any single or multi-tuned RF coil that resonates at frequency inside the two broadbands of the switch. One can change the coil without changing the switch. A dual tuned 1H/X-Nuclei or multi-tuned RF coil can be used with the same switch without any type of tuning. The introduced switch is a promising economical solution and can be used to minimize the needed space of T/R switches when multi-channel multi-tuned RF coils become widely available.

ACKNOWLEDGEMENT

This work has been done at the Department of Electrical Engineering, Faculty of Engineering and Technology at the Applied Science Private University, Amman, Jordan. The authors would like to thank the university for their strong support to this work.

REFERENCES

[1] K. Solbach, A. Abuelhaija, and S. Shooshtray, "Near-magnet power amplifier with built-in coil current sensing," in *Proceedings of the International Society for Magnetic Resonance in Medicine*, 2014, vol. 22.

[2] B. L. Edlow *et al.*, "7 Tesla MRI of the ex vivo human brain at 100 micron resolution," *Scientific Data*, vol. 6, no. 1, Dec. 2019, doi: 10.1038/s41597-019-0254-8.

[3] A. Laader *et al.*, "1.5 versus 3 versus 7 Tesla in abdominal MRI: a comparative study," *PLOS ONE*, vol. 12, no. 11, Nov. 2017, doi: 10.1371/journal.pone.0187528.

[4] T. J. Veersema *et al.*, "Seven tesla MRI improves detection of focal cortical dysplasia in patients with refractory focal epilepsy," *Epilepsia Open*, vol. 2, no. 2, pp. 162–171, Jun. 2017, doi: 10.1002/epi4.12041.

[5] L. Valkovič, M. Chmelík, and M. Krššák, "In-vivo 31P-MRS of skeletal muscle and liver: A way for non-invasive assessment of their metabolism," *Analytical Biochemistry*, vol. 529, pp. 193–215, 2017, doi: 10.1016/j.ab.2017.01.018.

[6] R. Hu, D. Kleimaier, M. Malzacher, M. A. U. Hoesl, N. K. Paschke, and L. R. Schad, "X-nuclei imaging: current state, technical challenges, and future directions," *Journal of Magnetic Resonance Imaging*, vol. 51, no. 2, pp. 355–376, 2020.

[7] S. C. Niesporek, A. M. Nagel, and T. Platt, "Multinuclear MRI at ultrahigh fields," *Topics in Magnetic Resonance Imaging*, vol. 28, no. 3, pp. 173–188, Jun. 2019, doi: 10.1097/RMR.0000000000000201.

[8] G. Madelin and R. R. Regatte, "Biomedical applications of sodium MRI in vivo," *Journal of Magnetic Resonance Imaging*, vol. 38, no. 3, pp. 511–529, 2013, doi: 10.1002/jmri.24168.

[9] M. Petracca, L. Fleysher, N. Oesingmann, and M. Inglese, "Sodium MRI of multiple sclerosis," *NMR in Biomedicine*, vol. 29, no. 2, pp. 153–161, Feb. 2016, doi: 10.1002/nbm.3289.

[10] J. Ren, A. D. Sherry, and C. R. Malloy, "31 P-MRS of healthy human brain: ATP synthesis, metabolite concentrations, pH, and T 1 relaxation times," *NMR in Biomedicine*, vol. 28, no. 11, pp. 1455–1462, Nov. 2015, doi: 10.1002/nbm.3384.

[11] D. W. J. Klomp *et al.*, "31P MRSI and 1H MRS at 7T: initial results in human breast cancer," *NMR in Biomedicine*, vol. 24, no. 10, pp. 1337–1342, 2011, doi: 10.1002/nbm.1696.

[12] B. W. J. Philips, M. J. Uden, S. H. G. Rietsch, S. Orzada, and T. W. J. Scheenen, "A multitransmit external body array combined with a 1 H and 31 P endorectal coil to enable a multiparametric and multimetabolic MRI examination of the prostate at 7T," *Medical Physics*, vol. 46, no. 9, pp. 3893–3905, Sep. 2019, doi: 10.1002/mp.13696.

[13] F. Du *et al.*, "Numerical simulation and evaluation of a four-channel-by-four-channel double-nuclear RF coil for 1H MRI and 31P MRSI at 7 T," in *IEEE Transactions on Magnetics*, vol. 54, no. 11, pp. 1-5, Nov. 2018, Art no. 5101105, doi: 10.1109/TMAG.2018.2856529.

[14] X. Yan, R. Xue, and X. Zhang, "A monopole/loop dual-tuned RF coil for ultrahigh field MRI," *Quantitative Imaging in Medicine and Surgery*, vol. 4, no. 4, pp. 225–31, 2014.

[15] D. O. Brunner *et al.*, "Symmetrically biased T/R switches for NMR and MRI with microsecond dead time," *Journal of Magnetic Resonance*, vol. 263, pp. 147–155, Feb. 2016, doi: 10.1016/j.jmr.2015.12.016.

[16] D. H. Johansen, M. M. Albannay, J. R. Petersen, V. Zhurbenko, and J. H. Ardenkjær-Larsen, "PIN diode driver for NMR and MRI," *Journal of Magnetic Resonance*, vol. 300, pp. 114–119, 2019, doi: 10.1016/j.jmr.2019.01.017.

[17] R. H. Caverly, "PIN diode-based transmit-receive switch for 7 T MRI," in *2016 IEEE Topical Conference on Biomedical Wireless Technologies, Networks, and Sensing Systems (BioWireleSS)*, Jan. 2016, pp. 100–102, doi: 10.1109/BIOWIRELESS.2016.7445574.

[18] R. H. Caverly, "PIN diode switching speed for MRI applications," in *2020 IEEE MTT-S International Microwave Biomedical Conference (IMBioC)*, Dec. 2020, pp. 1–3, doi: 10.1109/IMBIoC47321.2020.9385053.

[19] M. Twieg, M. Rooij, and M. Griswold, "Enhancement mode GaN on silicon (eGaN FETs) for coil detuning," *International Society for Magnetic Resonance in Medicine*, 2014.

[20] P. K. Grannell, M. J. Orchard, P. Mansfield, A. K. Garroway, and D. C. Stalker, "a fet analogue switch for pulsed Nmr receivers," *Journal of Physics E: Scientific Instruments*, vol. 6, no. 12, pp. 1202–1204, 1973, doi: 10.1088/0022-3735/6/12/020.

[21] H. Raki *et al.*, "Serial and parallel active decoupling characterization using RF MEMS switches for receiver endoluminal coils at 1.5 T," *IEEE Sensors Journal*, vol. 20, no. 18, pp. 10511–10520, 2020, doi: 10.1109/JSEN.2020.2995055.

[22] H. Raki *et al.*, "Serial and parallel active decoupling characterization using RF MEMS switches for receiver endoluminal coils at 1.5 T," *IEEE Sensors Journal*, vol. 20, no. 18, pp. 10511–10520, Sep. 2020, doi: 10.1109/JSEN.2020.2995055.

[23] A. Abuelhaija, G. Saleh, T. Baldawi, and S. Salama, "Symmetrical and asymmetrical microstripline-based trans-

mit/receive switches for 7-Tesla magnetic resonance imaging," *International Journal of Circuit Theory and Applications*, vol. 49, no. 7, pp. 2082–2093, 2021, doi: 10.1002/cta.3013.

[24] A. Abuelhaija, G. Saleh, S. Salama, and S. Issa, "T- and cascaded Pi-shaped 1H T/R switches with realistic trace width for 7 tesla MRI," *International Journal on Communications Antenna and Propagation (IRECAP)*, vol. 12, no. 1, Feb. 2022, doi: 10.15866/irecap.v12i1.21628.

[25] A. Abuelhaija, G. Saleh, O. Nashwan, S. Issa, and S. Salama, "Multi- and dual-tuned microstripline-based transmit/receive switch for 7-Tesla magnetic resonance imaging," *International Journal of Imaging Systems and Technology*, vol. 32, no. 2, pp. 590–599, Mar. 2022, doi: 10.1002/ima.22634.

[26] L. Chiu and Q. Xue, "Wideband parallel-strip 90° hybrid coupler with swap," *Electronics Letters*, vol. 44, no. 11, 2008, doi: 10.1049/el:20080975.

[27] L. Chiu and Q. Xue, "Investigation of a wideband 90° hybrid coupler with an arbitrary coupling level," *IEEE Transactions on Microwave Theory and Techniques*, vol. 58, no. 4, pp. 1022–1029, Apr. 2010, doi: 10.1109/TMTT.2010.2042835.

[28] M. Muraguchi, T. Yukitake, and Y. Naito, "Optimum design of 3-dB branch-line couplers using microstrip lines," *IEEE Transactions on Microwave Theory and Techniques*, vol. 31, no. 8, pp. 674–678, 1983, doi: 10.1109/TMTT.1983.1131568.

BIOGRAPHIES OF AUTHORS

Ashraf Abuelhaija is an Associate Professor in the Department of Electrical Engineering at Applied Science Private University, Amman, Jordan, where he received his BSc in communications and Electronics Engineering in 2007. He received his Master degree and Ph.D. in electrical engineering from Duisburg-Essen University in 2010 and 2016, respectively. His research interests are in the area of Antennas and RF technology. From 2012 to 2014, he works as research assistant at Erwin L. Hahn Institute for Magnetic Resonance Imaging, Essen, and from 2014 to 2016 as research assistant at the department of Microwave and RF technology at Duisburg-Essen University. He can be contacted at email: a_abualhijaa@asu.edu.jo.

Gameel Saleh was born in Aden, Yemen. He received the B.Sc. degree in Electrical Engineering from Aden University, Aden, Yemen, in 2001, the M.S. degree in Electrical Engineering from Jordan University of Science and Technology, Irbid, Jordan, in 2008, and the Dr.-Ing (Ph.D.) degree in Electrical Engineering from the Duisburg–Essen University, Duisburg, Germany, in December 2013. From 2014 to 2015, he worked at Aden University, Communication Engineering Department. From 2015 he is working as an associate professor with department of biomedical engineering at Imam Abdulrahman Bin Faisal University, Dammam, Saudi Arabia. His current research interests include RF circuits, metamaterials, wearable antennas, and biosensors. Dr. Saleh was a recipient of the German Academic Exchange Service Fellowships in 2006 and 2009. He can be contacted at email: gsmohammed@iau.edu.sa.